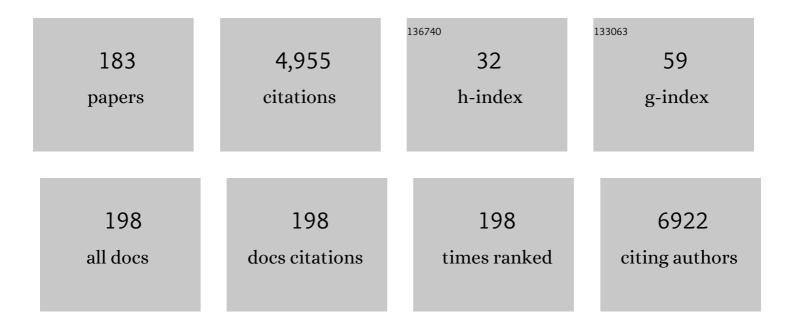
List of Publications by Year in descending order

Source: https://exaly.com/author-pdf/3459446/publications.pdf Version: 2024-02-01



ΖΗΙ ΥΛΝΟ

#	Article	IF	CITATIONS
1	Toward reliable characterization of functional homogeneity in the human brain: Preprocessing, scan duration, imaging resolution and computational space. NeuroImage, 2013, 65, 374-386.	2.1	428
2	Ultratough, Self-Healing, and Tissue-Adhesive Hydrogel for Wound Dressing. ACS Applied Materials & Interfaces, 2018, 10, 33523-33531.	4.0	381
3	An open science resource for establishing reliability and reproducibility in functional connectomics. Scientific Data, 2014, 1, 140049.	2.4	349
4	A Connectome Computation System for discovery science of brain. Science Bulletin, 2015, 60, 86-95.	4.3	129
5	Connectivity trajectory across lifespan differentiates the precuneus from the default network. Neurolmage, 2014, 89, 45-56.	2.1	128
6	Can Taichi Reshape the Brain? A Brain Morphometry Study. PLoS ONE, 2013, 8, e61038.	1.1	119
7	Individual Variability and Test-Retest Reliability Revealed by Ten Repeated Resting-State Brain Scans over One Month. PLoS ONE, 2015, 10, e0144963.	1.1	117
8	Abnormal baseline brain activity in bipolar depression: A resting state functional magnetic resonance imaging study. Psychiatry Research - Neuroimaging, 2012, 203, 175-179.	0.9	110
9	Toward neurobiological characterization of functional homogeneity in the human cortex: regional variation, morphological association and functional covariance network organization. Brain Structure and Function, 2015, 220, 2485-2507.	1.2	110
10	Genetic and Environmental Contributions to Functional Connectivity Architecture of the Human Brain. Cerebral Cortex, 2016, 26, 2341-2352.	1.6	100
11	Histologic subtype classification of non-small cell lung cancer using PET/CT images. European Journal of Nuclear Medicine and Molecular Imaging, 2021, 48, 350-360.	3.3	93
12	Tai Chi Chuan optimizes the functional organization of the intrinsic human brain architecture in older adults. Frontiers in Aging Neuroscience, 2014, 6, 74.	1.7	89
13	Ranking and averaging independent component analysis by reproducibility (RAICAR). Human Brain Mapping, 2008, 29, 711-725.	1.9	85
14	The self and its resting state in consciousness: An investigation of the vegetative state. Human Brain Mapping, 2014, 35, 1997-2008.	1.9	83
15	Pharmacokinetics and biodistribution of near-infrared fluorescence polymeric nanoparticles. Nanotechnology, 2009, 20, 165101.	1.3	81
16	Regional homogeneity of resting-state brain abnormalities in bipolar and unipolar depression. Progress in Neuro-Psychopharmacology and Biological Psychiatry, 2013, 41, 52-59.	2,5	68
17	Enhancing Anti-PD-1/PD-L1 Immune Checkpoint Inhibitory Cancer Therapy by CD276-Targeted Photodynamic Ablation of Tumor Cells and Tumor Vasculature. Molecular Pharmaceutics, 2019, 16, 339-348.	2.3	66
18	Clinical translational evaluation of Al18F-NOTA-FAPI for fibroblast activation protein-targeted tumour imaging. European Journal of Nuclear Medicine and Molecular Imaging, 2021, 48, 4259-4271.	3.3	64

#	Article	IF	CITATIONS
19	Clinical and Prognostic Value of PET/CT Imaging with Combination of ⁶⁸ Ga-DOTATATE and ¹⁸ F-FDG in Gastroenteropancreatic Neuroendocrine Neoplasms. Contrast Media and Molecular Imaging, 2018, 2018, 1-9.	0.4	58
20	Neural competition as a developmental process: Early hemispheric specialization for word processing delays specialization for face processing. Neuropsychologia, 2013, 51, 950-959.	0.7	57
21	Preclinical Evaluation and Pilot Clinical Study of Al ¹⁸ F-PSMA-BCH for Prostate Cancer PET Imaging. Journal of Nuclear Medicine, 2019, 60, 1284-1292.	2.8	56
22	First-in-Humans Evaluation of a PD-L1–Binding Peptide PET Radiotracer in Non–Small Cell Lung Cancer Patients. Journal of Nuclear Medicine, 2022, 63, 536-542.	2.8	56
23	68Ga-PSMA-617 PET/CT: a promising new technique for predicting risk stratification and metastatic risk of prostate cancer patients. European Journal of Nuclear Medicine and Molecular Imaging, 2018, 45, 1852-1861.	3.3	54
24	Brain Network Informed Subject Community Detection In Early-Onset Schizophrenia. Scientific Reports, 2014, 4, 5549.	1.6	48
25	⁶⁸ Ga-PSMA PET/CT Combined with PET/Ultrasound-Guided Prostate Biopsy Can Diagnose Clinically Significant Prostate Cancer in Men with Previous Negative Biopsy Results. Journal of Nuclear Medicine, 2020, 61, 1314-1319.	2.8	47
26	Altered resting-state cerebellar-cerebral functional connectivity in obsessive-compulsive disorder. Psychological Medicine, 2019, 49, 1156-1165.	2.7	46
27	Aberrant Functional Connectivity between the Amygdala and the Temporal Pole in Drug-Free Generalized Anxiety Disorder. Frontiers in Human Neuroscience, 2016, 10, 549.	1.0	44
28	Mechanisms and applications of bioinspired underwater/wet adhesives. Journal of Polymer Science, 2021, 59, 2911-2945.	2.0	42
29	Generalized RAICAR: Discover homogeneous subject (sub)groups by reproducibility of their intrinsic connectivity networks. Neurolmage, 2012, 63, 403-414.	2.1	41
30	Recent developments in multivariate pattern analysis for functional MRI. Neuroscience Bulletin, 2012, 28, 399-408.	1.5	41
31	Detecting Fibroblast Activation Proteins in Lymphoma Using ⁶⁸ Ga-FAPI PET/CT. Journal of Nuclear Medicine, 2022, 63, 212-217.	2.8	37
32	A prostate-specific membrane antigen activated molecular rotor for real-time fluorescence imaging. Nature Communications, 2021, 12, 5460.	5.8	37
33	A Highly Specific Multiple Enhancement Theranostic Nanoprobe for PET/MRI/PAI Imageâ€Guided Radioisotope Combined Photothermal Therapy in Prostate Cancer. Small, 2021, 17, e2100378.	5.2	35
34	Mind-Body Practice Changes Fractional Amplitude of Low Frequency Fluctuations in Intrinsic Control Networks. Frontiers in Psychology, 2017, 8, 1049.	1.1	34
35	Establishing Reliable Cu-64 Production Process: From Target Plating to Molecular Specific Tumor Micro-PET Imaging. Molecules, 2017, 22, 641.	1.7	33
36	Examination of Local Functional Homogeneity in Autism. BioMed Research International, 2015, 2015, 1-10.	0.9	32

#	Article	IF	CITATIONS
37	Insula shows abnormal taskâ€evoked and restingâ€state activity in firstâ€episode drugâ€naÃ⁻ve generalized anxiety disorder. Depression and Anxiety, 2020, 37, 632-644.	2.0	32
38	(<i>S</i>)-3-(Carboxyformamido)-2-(3-(carboxymethyl)ureido)propanoic Acid as a Novel PSMA Targeting Scaffold for Prostate Cancer Imaging. Journal of Medicinal Chemistry, 2020, 63, 3563-3576.	2.9	30
39	Individualized psychiatric imaging based on inter-subject neural synchronization in movie watching. NeuroImage, 2020, 216, 116227.	2.1	29
40	Evaluating early interim fluorine-18 fluorodeoxyglucose positron emission tomography/computed tomography with the SUV _{max-liver} -based interpretation for predicting the outcome in diffuse large B-cell lymphoma. Leukemia and Lymphoma, 2017, 58, 2065-2073.	0.6	26
41	Cerebellum engages in automation of verb-generation skill. Journal of Integrative Neuroscience, 2014, 13, 1-17.	0.8	25
42	Adaptive methylation regulation of <i>p53</i> pathway in sympatric speciation of blind mole rats, <i>Spalax</i> . Proceedings of the National Academy of Sciences of the United States of America, 2016, 113, 2146-2151.	3.3	25
43	Clinical Translation of a ⁶⁸ Ga-Labeled Integrin α _v β ₆ –Targeting Cyclic Radiotracer for PET Imaging of Pancreatic Cancer. Journal of Nuclear Medicine, 2020, 61, 1461-1467.	2.8	25
44	⁶⁸ Ga/ ¹⁷⁷ Lu-labeled DOTA-TATE shows similar imaging and biodistribution in neuroendocrine tumor model. Tumor Biology, 2017, 39, 101042831770551.	0.8	24
45	Development of a novel albumin-based and maleimidopropionic acid-conjugated peptide with prolonged half-life and increased <i>in vivo</i> anti-tumor efficacy. Theranostics, 2018, 8, 2094-2106.	4.6	24
46	Higher accuracy of [68ÂGa]Ga-DOTA-FAPI-04 PET/CT comparing with 2-[18F]FDG PET/CT in clinical staging of NSCLC. European Journal of Nuclear Medicine and Molecular Imaging, 2022, 49, 2983-2993.	3.3	24
47	Construction of 124I-trastuzumab for noninvasive PET imaging of HER2 expression: from patient-derived xenograft models to gastric cancer patients. Gastric Cancer, 2020, 23, 614-626.	2.7	23
48	68Ga-NOTA-FAPI-04 PET/CT in a patient with primary gastric diffuse large B cell lymphoma: comparisons with [18F] FDG PET/CT. European Journal of Nuclear Medicine and Molecular Imaging, 2021, 48, 647-648.	3.3	23
49	Imaging Brain Metastasis Patients With 18F-(2S,4R)-4-Fluoroglutamine. Clinical Nuclear Medicine, 2018, 43, e392-e399.	0.7	22
50	Reliability map of individual differences reflected in inter-subject correlation in naturalistic imaging. NeuroImage, 2020, 223, 117277.	2.1	22
51	Dynamic PET/CT Imaging of 68Ga-FAPI-04 in Chinese Subjects. Frontiers in Oncology, 2021, 11, 651005.	1.3	22
52	ICAM-1 orchestrates the abscopal effect of tumor radiotherapy. Proceedings of the National Academy of Sciences of the United States of America, 2021, 118, .	3.3	22
53	64Cu-PSMA-617: A novel PSMA-targeted radio-tracer for PET imaging in gastric adenocarcinoma xenografted mice model. Oncotarget, 2017, 8, 74159-74169.	0.8	22
54	Effects of intermittent negative pressure on osteogenesis in human bone marrow-derived stroma cells. Journal of Zhejiang University: Science B, 2009, 10, 188-192.	1.3	21

#	Article	IF	CITATIONS
55	Can the SUV _{max-liver} -based interpretation improve prognostic accuracy of interim and posttreatment ¹⁸ F-FDG PET/CT in patients with diffuse large B-cell lymphoma?. Leukemia and Lymphoma, 2018, 59, 660-669.	0.6	21
56	Preparation and biological evaluation of 99mTc-N4IPA for single photon emission computerized tomography imaging of hypoxia in mouse tumor. European Journal of Medicinal Chemistry, 2013, 69, 223-231.	2.6	20
57	Synthesis of Site-Specific Radiolabeled Antibodies for Radioimmunotherapy via Genetic Code Expansion. Bioconjugate Chemistry, 2016, 27, 2460-2468.	1.8	20
58	Segregated precuneus network and default mode network in naturalistic imaging. Brain Structure and Function, 2019, 224, 3133-3144.	1.2	20
59	Evaluation of 124I-JS001 for hPD1 immuno-PET imaging using sarcoma cell homografts in humanized mice. Acta Pharmaceutica Sinica B, 2020, 10, 1321-1330.	5.7	20
60	Similar spatial patterns of neural coding of category selectivity in FFA and VWFA under different attention conditions. Neuropsychologia, 2012, 50, 862-868.	0.7	19
61	Gray matter volume showed dynamic alterations in methamphetamine users at 6 and 12 months abstinence: A longitudinal voxel-based morphometry study. Progress in Neuro-Psychopharmacology and Biological Psychiatry, 2018, 81, 350-355.	2.5	19
62	Impact of 68Ga-NOTA-MAL-MZHER2 PET imaging in advanced gastric cancer patients and therapeutic response monitoring. European Journal of Nuclear Medicine and Molecular Imaging, 2021, 48, 161-175.	3.3	19
63	18F-Boramino acid PET/CT in healthy volunteers and glioma patients. European Journal of Nuclear Medicine and Molecular Imaging, 2021, 48, 3113-3121.	3.3	19
64	Using fMRI to decode true thoughts independent of intention to conceal. NeuroImage, 2014, 99, 80-92.	2.1	18
65	Cortisol awakening response predicts intrinsic functional connectivity of the medial prefrontal cortex in the afternoon of the same day. NeuroImage, 2015, 122, 158-165.	2.1	18
66	Clinical Evaluation of ^{99m} Tc-Rituximab for Sentinel Lymph Node Mapping in Breast Cancer Patients. Journal of Nuclear Medicine, 2016, 57, 1214-1220.	2.8	18
67	Design, Synthesis, and Biological Evaluation of ⁶⁸ Ga-DOTA–PA1 for Lung Cancer: A Novel PET Tracer for Multiple Somatostatin Receptor Imaging. Molecular Pharmaceutics, 2018, 15, 619-628.	2.3	18
68	Noninvasive Detection of HER2 Expression in Gastric Cancer by ⁶⁴ Cu-NOTA-Trastuzumab in PDX Mouse Model and in Patients. Molecular Pharmaceutics, 2018, 15, 5174-5182.	2.3	18
69	PET Imaging of ¹⁸ F-(2 <i>S</i> ,4 <i>R</i>)4-Fluoroglutamine Accumulation in Breast Cancer: From Xenografts to Patients. Molecular Pharmaceutics, 2018, 15, 3448-3455.	2.3	18
70	Construction of Anti-hPD-L1 HCAb Nb6 and <i>in Situ</i> ¹²⁴ I Labeling for Noninvasive Detection of PD-L1 Expression in Human Bone Sarcoma. Bioconjugate Chemistry, 2019, 30, 2614-2623.	1.8	18
71	Altered Negative Unconscious Processing in Major Depressive Disorder: An Exploratory Neuropsychological Study. PLoS ONE, 2011, 6, e21881.	1.1	17
72	The Correlation Between [68Ga]DOTATATE PET/CT and Cell Proliferation in Patients With GEP-NENs. Molecular Imaging and Biology, 2019, 21, 984-990.	1.3	17

#	Article	IF	CITATIONS
73	Synthesis, preclinical evaluation, and a pilot clinical imaging study of [18F]AlF-NOTA-JR11 for neuroendocrine neoplasms compared with [68Ga]Ga-DOTA-TATE. European Journal of Nuclear Medicine and Molecular Imaging, 2021, 48, 3129-3140.	3.3	17
74	Molecular PET/CT Profiling of ACE2 Expression In Vivo: Implications for Infection and Outcome from SARSâ€CoVâ€2. Advanced Science, 2021, 8, e2100965.	5.6	17
75	Amplitude of low-frequency fluctuations in first-episode, drug-naÃ⁻ve depressive patients: A 5-year retrospective study. PLoS ONE, 2017, 12, e0174564.	1.1	17
76	Investigating Brain Connectomic Alterations in Autism Using the Reproducibility of Independent Components Derived from Resting State Functional MRI Data. Frontiers in Neuroscience, 2017, 11, 459.	1.4	16
77	68Ga-labeled ODAP-Urea-based PSMA agents in prostate cancer: first-in-human imaging of an optimized agent. European Journal of Nuclear Medicine and Molecular Imaging, 2022, 49, 1030-1040.	3.3	16
78	Chemokine ligand 2 in the trigeminal ganglion regulates pain induced by experimental tooth movement. Angle Orthodontist, 2014, 84, 730-736.	1.1	15
79	Synthesis and radiolabeling of 1111n-core-cross linked polymeric micelle-octreotide for near-infrared fluoroscopy and single photon emission computed tomography imaging. Bioorganic and Medicinal Chemistry Letters, 2014, 24, 2781-2785.	1.0	15
80	Noninvasive small-animal imaging of galectin-1 upregulation for predicting tumor resistance to radiotherapy. Biomaterials, 2018, 158, 1-9.	5.7	15
81	Functional Connectivity Between Sensory-Motor Subnetworks Reflects the Duration of Untreated Psychosis and Predicts Treatment Outcome of First-Episode Drug-NaÃ`ve Schizophrenia. Biological Psychiatry: Cognitive Neuroscience and Neuroimaging, 2019, 4, 697-705.	1.1	15
82	Development of a psychological first-aid model in inpatients with COVID-19 in Wuhan, China. Annals of General Psychiatry, 2020, 33, e100292.	1.1	15
83	Limbic cortico-striato-thalamo-cortical functional connectivity in drug-naÃ ⁻ ve patients of obsessive-compulsive disorder. Psychological Medicine, 2021, 51, 70-82.	2.7	15
84	Adolescent anxiety disorders and the developing brain: comparing neuroimaging findings in adolescents and adults. Annals of General Psychiatry, 2021, 34, e100411.	1,1	15
85	Synthesis and radiolabeling of 64Cu-labeled 2-nitroimidazole derivative 64Cu-BMS2P2 for hypoxia imaging. Bioorganic and Medicinal Chemistry Letters, 2016, 26, 1397-1400.	1.0	14
86	Targeting CAIX with [⁶⁴ Cu]XYIMSR-06 Small Molecular Radiotracer Enables Noninvasive PET Imaging of Malignant Glioma in U87 MG Tumor Cell Xenograft Mice. Molecular Pharmaceutics, 2019, 16, 1532-1540.	2.3	14
87	Segregation between the parietal memory network and the default mode network: effects of spatial smoothing and model order in ICA. Science Bulletin, 2016, 61, 1844-1854.	4.3	14
88	Voxel-based morphometry study of the insular cortex in bipolar depression. Psychiatry Research - Neuroimaging, 2014, 224, 89-95.	0.9	13
89	Brain structure–function associations identified in large-scale neuroimaging data. Brain Structure and Function, 2016, 221, 4459-4474.	1.2	13
90	Altered gray matter volume and structural co-variance in adolescents with social anxiety disorder: evidence for a delayed and unsynchronized development of the fronto-limbic system. Psychological Medicine, 2021, 51, 1742-1751.	2.7	13

#	Article	IF	CITATIONS
91	Synthesis and Bioevaluation of Novel [¹⁸ F]FDG-Conjugated 2-Nitroimidazole Derivatives for Tumor Hypoxia Imaging. Molecular Pharmaceutics, 2019, 16, 2118-2128.	2.3	12
92	Metformin Reduces Renal Uptake of Radiotracers and Protects Kidneys from Radiation-Induced Damage. Molecular Pharmaceutics, 2019, 16, 808-815.	2.3	12
93	Dynamic PET/CT imaging of 18F-(2S, 4R)4-fluoroglutamine in healthy volunteers and oncological patients. European Journal of Nuclear Medicine and Molecular Imaging, 2020, 47, 2280-2292.	3.3	12
94	Production, quality control of next-generation PET radioisotope iodine-124 and its thyroid imaging. Journal of Radioanalytical and Nuclear Chemistry, 2018, 318, 1999-2006.	0.7	11
95	Excellent Response to 177Lu-DOTATATE Peptide Receptor Radionuclide Therapy in a Patient With Progressive Metastatic Castration-Resistant Prostate Cancer With Neuroendocrine Differentiation After 177Lu-PSMA Therapy. Clinical Nuclear Medicine, 2019, 44, 876-878.	0.7	11
96	Evaluation of 64Cu radiolabeled anti-hPD-L1 Nb6 for positron emission tomography imaging in lung cancer tumor mice model. Bioorganic and Medicinal Chemistry Letters, 2020, 30, 126915.	1.0	11
97	The Value of 18F-FDG PET/CT and Abdominal PET/MRI as a One-Stop Protocol in Patients With Potentially Resectable Colorectal Liver Metastases. Frontiers in Oncology, 2021, 11, 714948.	1.3	11
98	Metabolic characteristics of [18F]fluoroboronotyrosine (FBY) PET in malignant brain tumors. Nuclear Medicine and Biology, 2022, 106-107, 80-87.	0.3	11
99	Loss of Parietal Memory Network Integrity in Alzheimer's Disease. Frontiers in Aging Neuroscience, 2019, 11, 67.	1.7	10
100	Abnormal asymmetry of thalamic volume moderates stress from parents and anxiety symptoms in children and adolescents with social anxiety disorder. Neuropharmacology, 2020, 180, 108301.	2.0	10
101	64Cu-PSMA-BCH: a new radiotracer for delayed PET imaging of prostate cancer. European Journal of Nuclear Medicine and Molecular Imaging, 2021, 48, 4508-4516.	3.3	10
102	Metabolic radiolabeling and in vivo PET imaging of cytotoxic T lymphocytes to guide combination adoptive cell transfer cancer therapy. Journal of Nanobiotechnology, 2021, 19, 175.	4.2	10
103	Targeting Claudin 18.2 Using a Highly Specific Antibody Enables Cancer Diagnosis and Guided Surgery. Molecular Pharmaceutics, 2022, 19, 3530-3541.	2.3	10
104	Atrophy of hippocampal subfield CA2/3 in healthy elderly men is related to educational attainment. Neurobiology of Aging, 2019, 80, 21-28.	1.5	9
105	(2S,4R)-4-[18F]Fluoroglutamine as a PET Indicator for Bone Marrow Metabolism Dysfunctional: from Animal Experiments to Clinical Application. Molecular Imaging and Biology, 2019, 21, 945-953.	1.3	9
106	Noninvasive evaluation of PD-L1 expression using Copper 64 labeled peptide WL12 by micro-PET imaging in Chinese hamster ovary cell tumor model. Bioorganic and Medicinal Chemistry Letters, 2021, 40, 127901.	1.0	9
107	Synthesis and evaluation of (68)Ga-labeled DOTA-2-deoxy-D-glucosamine as a potential radiotracer in μPET imaging. American Journal of Nuclear Medicine and Molecular Imaging, 2012, 2, 499-507.	1.0	9
108	Radiolabeling and evaluation of (64)Cu-DOTA-F56 peptide targeting vascular endothelial growth factor receptor 1 in the molecular imaging of gastric cancer. American Journal of Cancer Research, 2015, 5, 3301-10.	1.4	9

#	Article	IF	CITATIONS
109	Synthesis and evaluation of 111In-labeled d-glucose as a potential SPECT imaging agent. Journal of Radioanalytical and Nuclear Chemistry, 2013, 295, 1371-1375.	0.7	8
110	ADAM10 is essential for cranial neural crest-derived maxillofacial bone development. Biochemical and Biophysical Research Communications, 2016, 475, 308-314.	1.0	8
111	Development of 99mTc-conjugated JS001 antibody for in vivo mapping of PD-1 distribution in murine. Bioorganic and Medicinal Chemistry Letters, 2019, 29, 2178-2181.	1.0	8
112	Parietal memory network and default mode network in firstâ€episode drugâ€naÃ⁻ve schizophrenia: Associations with auditory hallucination. Human Brain Mapping, 2020, 41, 1973-1984.	1.9	8
113	Development and validation of a kit formulation of [68Ga]Ga-P15-041 as a bone imaging agent. Applied Radiation and Isotopes, 2021, 169, 109485.	0.7	8
114	Diagnostic Value of Delayed PET/MR in Liver Metastasis in Comparison With PET/CT. Frontiers in Oncology, 2021, 11, 717687.	1.3	8
115	Comparing the Effectiveness of Brain Structural Imaging, Resting-state fMRI, and Naturalistic fMRI in Recognizing Social Anxiety Disorder in Children and Adolescents. Psychiatry Research - Neuroimaging, 2022, 323, 111485.	0.9	8
116	Novel 18F-Labeled 1-Hydroxyanthraquinone Derivatives for Necrotic Myocardium Imaging. ACS Medicinal Chemistry Letters, 2017, 8, 191-195.	1.3	7
117	125I–F56 Peptide as Radioanalysis Agent Targeting VEGFR1 in Mice Xenografted with Human Gastric Tumor. ACS Medicinal Chemistry Letters, 2017, 8, 266-269.	1.3	7
118	Connecting Openness and the Resting-State Brain Network: A Discover-Validate Approach. Frontiers in Neuroscience, 2018, 12, 762.	1.4	7
119	Characteristic properties of muscular-derived extracellular matrix and its application in rat abdominal wall defects. Regenerative Medicine, 2018, 13, 503-517.	0.8	7
120	Training the next generation of radiopharmaceutical scientists. Nuclear Medicine and Biology, 2020, 88-89, 10-13.	0.3	7
121	Improve cognition of depressive patients through the regulation of basal ganglia connectivity: Combined medication using Shuganjieyu capsule. Journal of Psychiatric Research, 2020, 123, 39-47.	1.5	7
122	Positron Emission Tomography Imaging of Programmed Death 1 Expression in Cancer Patients Using 124I-Labeled Toripalimab. Clinical Nuclear Medicine, 2021, 46, 382-388.	0.7	7
123	Pretherapeutic Assessment of Pancreatic Cancer: Comparison of FDG PET/CT Plus Delayed PET/MR and Contrast-Enhanced CT/MR. Frontiers in Oncology, 2021, 11, 790462.	1.3	7
124	Value of 18F-FDG PET/MRI in the Preoperative Assessment of Resectable Esophageal Squamous Cell Carcinoma: A Comparison With 18F-FDG PET/CT, MRI, and Contrast-Enhanced CT. Frontiers in Oncology, 2022, 12, 844702.	1.3	7
125	A self-triggered radioligand therapy agent for fluorescence imaging of the treatment response in prostate cancer. European Journal of Nuclear Medicine and Molecular Imaging, 2022, 49, 2693-2704.	3.3	7
126	Larger 18F-fluoroboronotyrosine (FBY) active volume beyond MRI contrast enhancement in diffuse gliomas than in circumscribed brain tumors. EJNMMI Research, 2022, 12, 22.	1.1	7

#	Article	IF	CITATIONS
127	Synthesis and evaluation of Cy5.5-Rit tracer for specific near-infrared fluorescence imaging of sentinel lymph node. Bioorganic and Medicinal Chemistry Letters, 2016, 26, 4233-4236.	1.0	6
128	Synthesis and bioevaluation of novel radioiodinated PEG-modified 2-nitroimidazole derivatives for tumor hypoxia imaging. Journal of Radioanalytical and Nuclear Chemistry, 2019, 321, 943-954.	0.7	6
129	Evaluation of a novel monoclonal antibody mAb109 by immuno-PET/fluorescent imaging for noninvasive lung adenocarcinoma diagnosis. Acta Pharmacologica Sinica, 2020, 41, 101-109.	2.8	6
130	Correlation and Comparison of Somatostatin Receptor Type 2 Immunohistochemical Scoring Systems with ⁶⁸ Ga-DOTATATE Positron Emission Tomography/Computed Tomography Imaging in Gastroenteropancreatic Neuroendocrine Neoplasms. Neuroendocrinology, 2022, 112, 358-369.	1.2	6
131	Development of an Albumin-Based PSMA Probe With Prolonged Half-Life. Frontiers in Molecular Biosciences, 2020, 7, 585024.	1.6	6
132	SARS-CoV-2 receptor binding domain radio-probe: a non-invasive approach for angiotensin-converting enzyme 2 mapping in mice. Acta Pharmacologica Sinica, 2022, 43, 1749-1757.	2.8	6
133	Synthesis and biological evaluation of ⁶⁸ Gaâ€labeled Pteroylâ€Lys conjugates for folate receptorâ€targeted tumor imaging. Journal of Labelled Compounds and Radiopharmaceuticals, 2016, 59, 346-353.	0.5	5
134	Analysis and prediction of team performance based on interaction networks. , 2017, , .		5
135	The correlation between molecular pathological profiles and metabolic parameters of 18F-FDG PET/CT in patients with gastroesophageal junction cancer. Abdominal Radiology, 2020, 45, 312-321.	1.0	5
136	Imaging superiority of [68Ga]-FAPI-04 over [18F]-FDG PET/CT in alveolar soft part sarcoma (ASPS). European Journal of Nuclear Medicine and Molecular Imaging, 2021, 48, 3741-3742.	3.3	5
137	First-in-human DR5 PET reveals insufficient DR5 expression in patients with gastrointestinal cancer. , 2021, 9, e002926.		5
138	Changes in plasma HDL and its subcomponents HDL2b and HDL3 regulate inflammatory response by modulating SOCS1 signaling to affect severity degree and prognosis of sepsis. Infection, Genetics and Evolution, 2021, 91, 104804.	1.0	5
139	Technetium-99m-labeled rituximab for use as a specific tracer of sentinel lymph node biopsy: a translational research study. Oncotarget, 2016, 7, 38810-38821.	0.8	5
140	Prognostic value of pre- and post-transplantation 18F-fluorodeoxyglucose positron emission tomography results in non-Hodgkin lymphoma patients receiving autologous stem cell transplantation. Chinese Journal of Cancer Research: Official Journal of China Anti-Cancer Association, Beijing Institute for Cancer Research, 2017, 29, 561-571.	0.7	5
141	Galectin expression detected by 68Ga-galectracer PET as a predictive biomarker of radiotherapy resistance. European Journal of Nuclear Medicine and Molecular Imaging, 2022, , 1.	3.3	5
142	The role of PET molecular imaging in immune checkpoint inhibitor therapy in lung cancer: Precision medicine and visual monitoring. European Journal of Radiology, 2022, 149, 110200.	1.2	5
143	INCloud: integrated neuroimaging cloud for data collection, management, analysis and clinical translations. Annals of General Psychiatry, 2021, 34, e100651.	1.1	5
144	Radio-synthesis and mass spectrometry analysis of 68Ga-DKFZ-PSMA-617 for non-invasive prostate cancer PET imaging. Journal of Radioanalytical and Nuclear Chemistry, 2016, 309, 575.	0.7	4

#	Article	IF	CITATIONS
145	In vitro and in vivo evaluation of a 64Cu-labeled propylene amine oxime complex as a potential hypoxia imaging agent bearing two 3-nitrotriazole groups. Journal of Radioanalytical and Nuclear Chemistry, 2017, 314, 111-118.	0.7	4
146	Synthesis and preclinical evaluation of 68Ga-PSMA-BCH for prostate cancer imaging. Bioorganic and Medicinal Chemistry Letters, 2019, 29, 933-937.	1.0	4
147	68Ga-ZHER2 PET/CT Reveals HER2-Positive Metastatic Gastric Cancer With Better Image Quality Than 18F-FDG. Clinical Nuclear Medicine, 2020, 45, e101-e102.	0.7	4
148	Evaluation of Pan-SSTRs Targeted Radioligand [⁶⁴ Cu]NOTA-PA1 Using Micro-PET Imaging in Xenografted Mice. ACS Medicinal Chemistry Letters, 2020, 11, 445-450.	1.3	4
149	Impact of inter-individual variability on the estimation of default mode network in temporal concatenation group ICA. Neurolmage, 2021, 237, 118114.	2.1	4
150	Prognostic value of 18F-fluorodeoxyglucose positron emission tomography using Deauville criteria in diffuse large B cell lymphoma treated with autologous hematopoietic stem cell transplantation. Chinese Journal of Cancer Research: Official Journal of China Anti-Cancer Association, Beijing Institute for Cancer Research, 2019, 31, 162-170.	0.7	4
151	Evaluating [68Ga]Ga-p14-032 as a Novel PET Tracer for Diagnosis Cerebral Amyloid Angiopathy. Frontiers in Neurology, 2021, 12, 702185.	1.1	4
152	68Ga-P15-041, A Novel Bone Imaging Agent for Diagnosis of Bone Metastases. Frontiers in Oncology, 2021, 11, 766851.	1.3	4
153	An Albumin-Binding PSMA Ligand with Higher Tumor Accumulation for PET Imaging of Prostate Cancer. Pharmaceuticals, 2022, 15, 513.	1.7	4
154	Evaluation of 1111n-DOTA-F56 peptide targeting VEGFR1 for potential non-invasive gastric cancer xenografted tumor mice Micro-SPECT imaging. Bioorganic and Medicinal Chemistry Letters, 2020, 30, 127248.	1.0	3
155	Production of the nextâ€generation positron nuclide zirconiumâ€89 (⁸⁹ Zr) guided by Monte Carlo simulation and its good quality for antibody labeling. Journal of Labelled Compounds and Radiopharmaceuticals, 2021, 64, 47-56.	0.5	3
156	Multimodal Imaging Technology Effectively Monitors HER2 Expression in Tumors Using Trastuzumab-Coupled Organic Nanoparticles in Patient-Derived Xenograft Mice Models. Frontiers in Oncology, 2021, 11, 778728.	1.3	3
157	Growth charts of brain morphometry for preschool children. NeuroImage, 2022, , 119178.	2.1	3
158	Enhance fMRI Data Analysis by RAICAR. , 2009, , .		2
159	Design and radio-synthesis of somatostatin receptors targeted 68Ga-DOTA-Benereotide for non-invasive PET imaging. Journal of Radioanalytical and Nuclear Chemistry, 2016, 307, 1069-1075.	0.7	2
160	ADAM10 modulates SOX9 expression <i>via</i> N1ICD during chondrogenesis at the cranial base. RSC Advances, 2018, 8, 38315-38323.	1.7	2
161	Initial experience in synthesis of (<scp>2<i>S</i></scp> , <scp>4<i>R</i></scp>)â€4â€{ ¹⁸ F]fluorog utamine for clinical application. Journal of Labelled Compounds and Radiopharmaceuticals, 2019, 62, 209-214.	0.5	2
162	DisConICA: a Software Package for Assessing Reproducibility of Brain Networks and their Discriminability across Disorders. Neuroinformatics, 2020, 18, 87-107.	1.5	2

#	Article	IF	CITATIONS
163	Construction and Preclinical Evaluation of a ^{124/131} I-Labeled Radiotracer for the Detection of Mesothelin-Overexpressing Cancer. Molecular Pharmaceutics, 2020, 17, 1875-1883.	2.3	2
164	Synthesis and evaluation of 64Cu-radiolabeled NOTA-cetuximab (64Cu-NOTA-C225) for immuno-PET imaging of EGFR expression. Chinese Journal of Cancer Research: Official Journal of China Anti-Cancer Association, Beijing Institute for Cancer Research, 2019, 31, 400-409.	0.7	2
165	Inferior Vena Cava Tumor Thrombus From Thyroid Cancer Detected by 68Ga-PSMA-617 PET/CT. Clinical Nuclear Medicine, 2021, 46, 264-265.	0.7	2
166	Evaluating the impact of different positron emitters on the performance of a clinical PET/MR system. Medical Physics, 2022, , .	1.6	2
167	Highlight selection of radiochemistry and radiopharmacy developments by editorial board. EJNMMI Radiopharmacy and Chemistry, 2021, 6, 13.	1.8	1
168	Influence of chelator and near-infrared dye labeling on biocharacteristics of dual-labeled trastuzumab-based imaging agents. Chinese Journal of Cancer Research: Official Journal of China Anti-Cancer Association, Beijing Institute for Cancer Research, 2016, 28, 362-369.	0.7	1
169	Application Analysis of 124I-PPMN for Enhanced Retention in Tumors of Prostate Cancer Xenograft Mice. International Journal of Nanomedicine, 2021, Volume 16, 7685-7695.	3.3	1
170	Optimization of ODAP-Urea-based dual-modality PSMA targeting probes for sequential PET-CT and optical imaging. Bioorganic and Medicinal Chemistry, 2022, 66, 116810.	1.4	1
171	Noninvasive Mapping of Angiotensin Converting Enzyme-2 in Pigeons Using Micro Positron Emission Tomography. Life, 2022, 12, 793.	1.1	1
172	¹²⁴ I Radiolabeled Basiliximab for CD25-Targeted Immuno-PET Imaging of Activated T Cells. Molecular Pharmaceutics, 2022, 19, 2629-2637.	2.3	1
173	Categorical and Dimensional Deficits in Hippocampal Subfields Among Schizophrenia, Obsessive-Compulsive Disorder, Bipolar Disorder, and Major Depressive Disorder. Biological Psychiatry: Cognitive Neuroscience and Neuroimaging, 2023, 8, 91-101.	1.1	1
174	The significance of radioimmunoimaging in the management of cancer patients. Chinese Journal of Cancer Research: Official Journal of China Anti-Cancer Association, Beijing Institute for Cancer Research, 1995, 7, 115-120.	0.7	0
175	Studies of99mTc labelled monoclonal antibody 3H11. Chinese Journal of Cancer Research: Official Journal of China Anti-Cancer Association, Beijing Institute for Cancer Research, 1995, 7, 187-192.	0.7	0
176	Can interpersonal hypersensitivity under subconscious condition explain paranoid symptom in schizophrenia?. Asia-Pacific Psychiatry, 2017, 9, e12221.	1.2	0
177	Analysis and Evaluation of Individual Performance in Team Task. , 2019, , .		0
178	Clinical Evaluation of MR-Gated Respiratory Motion Correction in Simultaneous PET/MRI. Clinical Nuclear Medicine, 2021, 46, 297-302.	0.7	0
179	Benign Adrenal Nodule Mimicking Lymphoma Differentially Diagnosed by 18F-FDG and 18F-FGIn PET/CT. Clinical Nuclear Medicine, 2021, 46, 474-476.	0.7	0
180	Correlation between NEN bone metastasis performance and tumor proliferation: 112 cases of [68Ga]Ga-DOTA-TATE results analysis. Neuroendocrinology, 2021, , .	1.2	0

#	Article	IF	CITATIONS
181	Initial evaluation of 99m Tcâ€labeled antiâ€carcinoembryonic antigen singleâ€chain fragment variable for microâ€singleâ€photon emission computed tomography imaging in mice with colorectal cancer. Journal of Labelled Compounds and Radiopharmaceuticals, 2021, , .	0.5	О
182	Risk Assessment in Diffuse Large B-Cell Lymphoma by Combining Baseline Metabolic Tumor Volume and Peking Criteria When Evaluating Series 18F-Fluorodeoxyglucose Positron Emission Tomography Scans. Frontiers in Oncology, 2022, 12, 876581.	1.3	0
183	The effect of a loading dose of meropenem on outcomes of patients with sepsis treated by continuous renal replacement: study protocol for a randomized controlled trial. Trials, 2022, 23, 294.	0.7	ο